HHS Public Access

Author manuscript

Nat Med. Author manuscript; available in PMC 2014 April 11.

Published in final edited form as:

Nat Med. 2013 April ; 19(4): 429–436. doi:10.1038/nm.3057.

CD169+ macrophages provide a niche promoting erythropoiesis under homeostasis, myeloablation and in JAK2V617F-induced polycythemia vera

Andrew Chow[1,2,3], **Matthew Huggins**[3], **Jalal Ahmed**[1,2,3], **Daigo Hashimoto**[1,2], **Daniel Lucas**[3], **Yuya Kunisaki**[3], **Sandra Pinho**[3], **Marylene Leboeuf**[1,2], **Clara Noizat**[1,2,5], **Nico van Rooijen**[6], **Masato Tanaka**[7,8], **Zhizhuang Joe Zhao**[9], **Aviv Bergman**[4], **Miriam Merad**[1,2,*], and **Paul S. Frenette**[3,*]

[1]Mount Sinai School of Medicine, Departments of Oncological Sciences, New York, NY 10029, USA [2]Department of Medicine, New York, NY 10029, USA [3]Ruth L. and David S. Gottesman Institute for Stem Cell and Regenerative Medicine Research, Bronx, NY 10461, USA [4]Department of Systems & Computational Biology, Albert Einstein College of Medicine, Bronx, NY 10461, USA [5]Universite Pierre at Marie Curie, Paris, France [6]Department of Molecular Cell Biology, Vrije Universiteit, Amsterdam, The Netherlands [7]Laboratory for Innate Cellular Immunity, RIKEN Research Center for Allergy and Immunology, Yokohama, Kanagawa, Japan [8]Laboratory of Immune Regulation, School of Life Science, Tokyo University of Pharmacy and Life Sciences, Hachiouji, Tokyo, Japan [9]Department of Pathology, University of Oklahoma Health Sciences Center, Oklahoma City, OK 73104

Abstract

The role of macrophages in erythropoiesis was suggested several decades ago with the description of “erythroblastic islands” in the bone marrow (BM) composed of a central macrophage surrounded by developing erythroblasts. However, the *in vivo* role of macrophages in erythropoiesis under homeostasis or disease remains unclear. Specific depletion of $CD169^+$ macrophages markedly reduced erythroblasts in the BM but did not result in overt anemia under homeostasis likely due to concomitant alterations in RBC clearance. However, $CD169^+$ macrophage depletion significantly impaired erythropoietic recovery from hemolytic anemia, acute blood loss and myeloablation. Furthermore, macrophage depletion normalized the erythroid compartment in a $JAK2^{V617F}$-driven murine model of polycythemia vera (PV), suggesting that erythropoiesis in PV, unexpectedly, remains under the control of macrophages in the BM and splenic microenvironments. These data indicate that $CD169^+$ macrophages promote late erythroid

Correspondence should be addressed to paul.frenette@einstein.yu.edu or miriam.merad@mssm.edu.

*These authors contributed equally to this work.

Author Contributions

A.C. designed the experiments, conducted experiments, analysed data, and wrote the manuscript. M.M. and P.S.F. designed the experiments and wrote the manuscript. M.H., J.A., D.H., D.L., Y.K., S.P., M.L., and C.N. conducted experiments, analysed data, and provided feedback on the manuscript. N.vR provided clodronate liposomes and feedback on the manuscript. M.T., Z.J.Z. provided mice and feedback on the manuscript. A.B. designed the mathematical model of steady-state erythropoiesis and provided feedback on the manuscript.

maturation and that modulation of the macrophage compartment represents a novel strategy to treat erythropoietic disorders.

Humans produce millions of erythrocytes each minute and careful coordination of production and clearance are critical to maintain erythropoietic homeostasis. This homeostasis can be particularly challenged by a number of genetic (e.g. sickle cell disease, thalassemia, polycythemia vera), infectious (e.g. malaria, parvovirus), exposure (e.g. lead, radiation, trauma-induced blood loss), and iatrogenic (e.g. chemotherapy, bone marrow transplant) perturbations.

In 1958, Marcel Bessis proposed that erythropoietic maturation required a specific microenvironment comprised of a nursing macrophage decorated by erythroblasts at various stages of maturation, culminating with enucleation[1]. A functional role for these erythroblastic islands was first demonstrated by Narla and colleagues when they showed that hypertransfused animals had a substantial reduction in the number of islands quantified by tridimensional electron microscopy[2]. A supportive role of macrophages in erythroblast development was strengthened by *in vitro* observations that macrophages promote erythroblast proliferation and survival[3–5] and an extensive amount of work has been done to characterize the adhesive interactions within these islands (reviewed in [6]). Nonetheless, whether macrophages contribute to erythropoiesis *in vivo* remains to be elucidated.

We have recently reported that murine BM macrophages express CD169 (also known as Sialoadhesin or Siglec-1)[7,8] and that these macrophages can be selectively depleted in CD169-DTR mice, which express the human diphtheria toxin receptor (DTR) knocked-in downstream of the endogenous *Siglec1* promoter[9]. Since central macrophages in erythroblastic islands reportedly express CD169[10], we sought to re-examine the role of macrophages in steady-state erythropoiesis *in vivo*. Moreover, we assessed the contribution of BM and splenic macrophages to the recovery from erythropoietic stress and also to the hyperfunctional erythron observed in JAK2^{V617}-induced polycythemia vera.

RESULTS

CD169^{+} macrophage depletion reduces bone marrow erythroblasts, but does not result in peripheral blood anemia

To examine the role of BM macrophages in erythroblast formation, we utilized heterozygous CD169-DTR (CD169$^{DTR/+}$) animals. We observed that after sustained diphtheria toxin (DT) administration and ensuing depletion of BM CD169^{+} macrophages, but not monocytes[7,8], long bones were paler than that of control animals (Fig. 1a), and this was associated with a >60% reduction in the number of F4/80^{+}Ter119^{+} erythroblast islands (Fig. 1b and Supplementary Fig. 1). We also observed that sustained depletion of CD169^{+} macrophages (Fig. 1c) resulted in a reduction in erythroblasts in the BM at various time points after initiation of depletion, starting as early as 12h post DT administration (with two gating schemes: Fig. 1c–e and Supplementary Fig. 2a,b). This reduction in BM erythroblasts was observed across all stages of maturation (Supplementary Fig. 2c–e). Cultured erythroblasts from CD169$^{DTR/+}$ mice were unaffected by DT administration (Supplementary Fig. 2f,g),

whereas cultured macrophages were susceptible at the same dose ([7] and data not shown), ruling out a direct depletion of erythroblasts. Consistent with the flow cytometry data, we observed a ~50% reduction in CFU-E, but not BFU-E, in the BM 24h after DT administration (Supplementary Fig. 2h,i), which is consistent with the notion that macrophages are important for the BM erythroblast stages starting with the CFU-E/proerythroblasts[6,11]. The reduction of erythroblasts was not due to lower proliferation or viability (Supplementary Fig. 3). Our recent observation that $CD169^+$ macrophages control the retention of hematopoietic stem and progenitor cells in the BM[7] together with our finding that the reduction of BM $CD169^+$ macrophages and erythroblasts follow similar kinetics in the $CD169^{DTR/+}$ depletion model (Fig. 1c,e) led us to hypothesize that increased release of erythroblasts into the peripheral circulation might account for the erythroblast reduction in the BM. Indeed, 24h after initiation of $CD169^+$ macrophage depletion, we observed >2-fold increase in the number of erythroblasts in the peripheral blood (PB) (Supplementary Fig. 4a,b), which is consistent with a prior report[12]. Although PB erythroblasts were similarly viable (Supplementary Fig. 4c), they proliferated half as much as their BM counterparts (Supplementary Fig. 4d). This increased level of circulating peripheral EB is sustained after four weeks of depletion and all four subsets of EB are increased (Supplementary Fig. 4e–i). Since the spike in PB erythroblasts alone cannot account for the reduction observed in the BM, the erythroblasts are presumably mobilized to the spleen (Supplementary Fig. 5d,e) and other unexamined peripheral tissues. Thus, although BM $CD169^+$ macrophages do not regulate erythroblast proliferation or viability per se in the steady-state BM, they control their retention in the BM, which represents a major site for erythropoiesis.

Despite a reduction of BM erythroblasts, mice did not develop an overt peripheral blood anemia (Fig. 1f), consistent with previous reports utilizing clodronate liposomes[12,13]. $CD169^+$ macrophage-depleted animals did not have a compensatory increase in serum erythropoietin or hepatic erythroblastosis (Supplementary Fig. 5a–c). Although compensatory splenic erythroblastosis was present, splenectomized $CD169^+$ macrophage-depleted mice also did not develop overt anemia, indicating that splenic compensation was not sufficient to mask the BM production defect (Supplementary Fig. 5d–f). Along with BM macrophages, splenic red pulp macrophages (RPM) and hepatic Kupffer macrophages were also reduced after four weeks of sustained DT administration (Supplementary Fig. 5g–i). Consistent with the fact that the latter two populations are critical for the clearance of aged red blood cells (RBCs)[14], we observed that $CD169^+$ macrophage depletion resulted in a ~25% increase in RBC lifespan after 4 weeks, suggesting that abrogated clearance of aged RBCs was a mechanism parallel to splenic compensation that masked the reduction of BM erythroblasts in the steady state. We used mathematical modeling to assess whether the prolongation of RBC lifespan was sufficient to explain the absence of anemia after macrophage depletion. Since macrophages were involved in both the production and clearance of RBCs, the analysis suggested that peripheral RBC counts in the steady state are proportional to the ratio between the rates of production and clearance and independent of the absolute macrophage content (Supplementary Fig. 6).

Bone marrow and splenic macrophages are critical for recovery from hemolytic anemia and acute blood loss

Although no anemia developed from CD169$^+$ macrophage depletion in steady-state animals, we reasoned that we might be able to resolve a difference after erythropoietic stress. Indeed, in a model of hemolytic anemia induced by the hemoglobin-oxidizing toxin phenylhydrazine (PHZ), we observed a delay in reticulocytosis and hematocrit recovery in macrophage-depleted animals using both the CD169-DTR and clodronate liposome model which depletes most mononuclear phagocytes, including BM monocytes and CD169$^+$ macrophages[7] (Fig. 2a–d). Since clodronate liposomes appeared to more dramatically impair the recovery from hemolytic anemia compared to the CD169-DTR model, we reasoned that this could be due to differential capacity of the two models to deplete splenic RPM. Indeed, whereas both models efficiently depleted BM macrophages[7], short-term administration of DT did not result in a reduction in splenic RPM (Supplementary Fig. 7a). This is consistent with a prior report[9] and in contrast with the reduction observed after four weeks of DT administration (Supplementary Fig. 5h).

Pre-treatment of clodronate liposomes five days prior to the administration of PHZ reduced macrophage numbers and impaired recovery of erythroblasts in the BM and spleen (Supplementary Fig. 7b–e). Moreover, macrophage depletion reduced splenic BMP4 induction and the number of splenic stress BFU-E (Supplementary Fig. 7f–g). The impairment in hematocrit recovery from PHZ challenge, albeit more modest in the CD169-DTR model, suggested that BM erythropoiesis made a functional contribution to recovery from hemolytic anemia, along with their splenic stress counterparts. To further ascertain the contribution of BM erythropoiesis, we compared recovery of control and CD169$^+$ macrophage-depleted splenectomized mice. We observed that although hematopoietic recovery was slower compared to non-splenectomized animals (Fig. 2b,f), CD169$^+$ macrophage-depleted animals still demonstrated a hampered recovery (Fig. 2e,f). Consistent with the PHZ model and a prior report[15], macrophage-depleted animals also demonstrated a substantial impairment in recovery from acute blood loss (Fig. 2g,h). Hence, in two models of acute RBC reduction, macrophages are essential for efficient recovery.

Radioresistant splenic red pulp macrophages are critical for BMP4-dependent stress erythropoiesis and erythroid recovery following myeloablation

To test whether CD169$^+$ macrophages could also contribute to erythroid recovery from myeloablation, we depleted mice after bone marrow transplantation (BMT). BMT itself reduced the number of BM CD169$^+$ macrophages and erythroblasts seven days after BMT (Fig. 3a,b), and the reduction in erythroblasts was even more profound when CD169$^+$ macrophages were depleted following BMT (Fig. 3b). Moreover, CD169$^+$ macrophage depletion post-BMT severely abrogated the recovery of splenic erythroblasts (Fig. 3c,d). Thus, in the context of myeloablation, splenic RPM are efficiently depleted by short-term DT administration in the CD169-DTR model. CD169$^+$ macrophage depletion also delayed reticulocytosis and hematocrit recovery (Fig. 3e,f), indicating the functional peripheral consequences of impaired erythroblast recovery. CD169$^+$ macrophage depletion was similarly associated with delayed erythroblast and peripheral erythrocyte recovery following challenge with the myeloablative agent 5-fluorouracil (5FU) (Supplementary Fig. 8a–g).

Interestingly, in both BMT and 5FU models, CD169$^+$ macrophage-depleted animals had less severe early declines in hematocrit (Fig. 3f and Supplementary Fig. 8g). This suggests that myeloablation-induced pathogenic consumption of mature RBC by macrophages may contribute to anemia following clastogenic injury, which we confirmed by observing that RBCs had a longer half-life in CD169$^+$ macrophage-depleted animals shortly after BMT (Supplementary Fig. 8h). Together, these results indicate that similar to the steady state, CD169$^+$ macrophages promote both the production and destruction of erythrocytes. Nonetheless, the supportive role of CD169$^+$ macrophages in erythroid production is both dominant and essential for efficient recovery from myeloablation.

It was initially hypothesized that macrophages may represent nurse-like cells providing iron to developing RBC[16] and since then, macrophage regulation of iron homeostasis has been well-documented[17]. We analyzed serum iron, transferrin saturation, mean corpuscular hemoglobin (MCH), and reticulocyte hemoglobin content (CHr) in the steady state or following BMT to evaluate the potential effect of CD169$^+$ macrophage depletion on iron homeostasis in erythrocytes. In the steady state, CD169$^+$ macrophage depletion reduced serum iron, transferrin saturation, MCH and CHr after 3–4 weeks of sustained depletion (Supplementary Fig. 9a–d). This delayed effect is more consistent with compromised ferroportin-mediated systemic iron recycling by macrophages[18], rather than a local nurse-like function. In the context of erythropoietic challenge from BMT, we did not observe any significant changes in serum iron or transferrin saturation 7d after transplant and MCH did not show a reduction until the third week post-BMT; however, a reduction in CHr could be observed by seven days following BMT (Supplementary Fig. 9e–h), suggesting a local role of tissue macrophages in iron homeostasis in the early recovery from myeloablation, which is consistent with a local nurse-like role. Systemic administration of iron dextran did not rescue the impaired erythropoietic recovery observed in CD169$^+$ macrophage-depleted animals (Supplementary Fig. 9i,j). Although these data do not preclude a local role of macrophage-derived iron in the observed deficits, they do suggest that macrophages alter the erythron through additional mechanisms.

Since BMP4 promotes the development of stress erythroid progenitors following BMT[19,20], we assessed whether induction of splenic BMP4 was reduced in CD169$^+$ macrophage-depleted animals. Indeed, we found that splenic induction of BMP4 and stress BFU-E was abrogated in CD169$^+$ macrophage-depleted animals (Fig. 3g,h). Splenic RPM are radioresistant compared to other hematopoietic populations[21,22] and have been previously implicated as the source of BMP4[23]. Since 90% of splenic RPM remained of host origin seven days after BMT (Supplementary Fig. 9k), we assessed whether depletion of host-derived splenic RPM was sufficient to abrogate erythropoietic recovery by performing reciprocal BMT between WT and CD169$^{DTR/+}$ animals and treating all mice with DT. CD169$^{DTR/+}$ animals transplanted with WT BM cells (WT→DTR) demonstrated similar levels of depletion of splenic RPM compared to those transplanted with CD169$^{DTR/+}$ BM cells (DTR→DTR), confirming the predominance of host-derived RPM seven days after BMT (Supplementary Fig. 9l). Importantly, WT→DTR animals also had impaired recovery of splenic erythroblasts and stress BFU-E (Fig. 3i,j). Taken together, BMP4 derived from radioresistant, host-derived splenic RPM is critical for erythroid recovery following myeloablation.

Abrogation of VCAM1 impairs erythropoietic recovery following myeloablation

Vascular cell adhesion molecule 1 (VCAM1) has previously been demonstrated to play a role in erythroblast island interactions *in vitro*[24]. Gene expression profiling of purified BM mononuclear phagocytes revealed that the expression of *Vcam1* transcripts was significantly higher on BM CD169^{+} macrophages compared to BM Gr1^{hi} or Gr1^{lo} monocytes (Supplementary Fig. 10a). Consistently, monocytes expressed low VCAM1 levels on the cell surface, whereas both BM and splenic RPM[25] expressed abundant levels of VCAM1 (Fig. 4a and Supplementary Fig. 10b). In addition, cell-surface levels of VCAM1 were reduced in the BM of CD169^{+} macrophage-depleted mice in the steady state (Supplementary Fig. 10c) and seven days post-BMT (Fig. 4b). In line with the role of radioresistant host-derived macrophages in the spleen, we also observed that depletion of radioresistant (Supplementary Fig. 10d) host-derived BM CD169^{+} macrophages in the reciprocal BMT model was sufficient to reduce CD169^{+} macrophages, VCAM1 levels, and erythroblasts in the BM (Fig. 4c–e). Importantly, anti-VCAM1 antibody administered in the post-BMT setting in macrophage-sufficient animals led to impaired recovery of BM erythroblasts, reticulocytes, and hematocrit, similar to macrophage-depleted animals (Fig. 4f–h). Notably, splenic VCAM1 levels were not dramatically reduced by CD169^{+} macrophage depletion and anti-VCAM1 antibody did not abrogate the development of splenic erythropoiesis (Supplementary Fig. 10e,f). These data suggests that VCAM1 expressed by CD169^{+} BM macrophages works in parallel with BMP4 derived from CD169^{+} splenic macrophages to promote erythroid recovery following myeloablation.

Human BM macrophages co-express CD169 and VCAM1

To determine whether human BM macrophages shared features with their murine counterparts, we performed phenotypic analysis of cells from the BM aspirate of healthy donors and assessed for CD169 and VCAM1 expression. CD15 is a marker of human granulocytes and monocytes[26] (Fig. 5a,b), and neither CD15^{+}CD14^{-} granulocytes nor CD15^{+}CD14^{+} monocytes expressed CD169 or VCAM1. CD163 is a marker of human monocytes and macrophages[27]. Within the CD15^{-}CD163^{+} population, a CD169^{+}VCAM1^{+} population with macrophage morphology was present (Fig. 5a,b and Supplementary Fig. 10g), whereas the CD169^{-} VCAM1^{-} population appeared to have a monocytic morphology. Therefore, like their murine counterparts, human BM macrophages can also be identified by CD169 and VCAM1 expression.

Macrophage depletion normalizes the erythron in JAK2^{V617F}-mediated polycythemia vera

Having demonstrated the role of macrophages in recovery after erythropoietic insufficiency, we sought to determine whether macrophage depletion could be beneficial in the context of an overactive erythron and tested the effect of depletion in a model of polycythemia vera (PV). We hypothesized that even when driven by an oncogenic mutation, erythropoiesis might still respond to microenvironmental cues from its niche. To investigate this issue, we transplanted BM cells isolated from wild-type (WT) mice or transgenic mice harboring the JAK2^{V617F} mutation[28] into lethally irradiated wild-type mice. Increased reticulocytosis was already observed by day 9 post-BMT (Fig. 6a) and erythrocytosis was observed by day 16 post-BMT (Fig. 6b and Supplementary Fig. 11a), whereas WBC and platelet recovery were

not consistently different (Supplementary Fig. 11b,c). Five weeks after BMT, recipients of JAK2^{V617F} BM (PV mice) were infused weekly with PBS- or clodronate-encapsulated liposomes for 4 weeks. Macrophage depletion reduced erythroblasts in the BM and spleen (Fig. 6c–f), affecting all splenic erythroblast subsets (Supplementary Fig. 11d–g), and strikingly normalized blood hematocrit (Fig. 6g). The therapeutic benefit of macrophage depletion persisted for four weeks after the cessation of liposome treatment, and a single administration of clodronate liposomes was sufficient to reduce macrophages and erythroblasts in the BM and spleen (Supplementary Fig. 11h–k) and normalized the hematocrit for a shorter period than weekly administration (Supplementary Fig. 11l).

Macrophage depletion had a subtle effect on MCH, serum iron, and transferrin saturation in the PV model, but a rapid effect on CHr (Supplementary Fig. 12a–d). Although treatment of PV mice with the iron chelating agent deferoxamine reduced serum iron levels (Supplementary Fig. 12c), it neither reduced splenic erythroblast numbers nor hematocrit (Supplementary Fig. 12e,f). Hence global alterations in iron are not the mechanism by which macrophage depletion suppresses PV, although this does not necessarily rule out a local microenvironmental effect.

Since splenic erythropoiesis was reduced by macrophage depletion, we hypothesized that JAK2^{V617F} mutation could potentially induce splenic stress erythropoiesis. Consistent with this hypothesis, we observed BMP4 and stress BFU-E induction in PV animals (Fig. 6h,i), and importantly, clodronate treatment abrogated this induction (Fig. 6h,i). Strikingly, we also observed that the number of EPO-independent endogenous erythroid colonies, a clinical criterion of JAK2^{V617F}-induced PV[29], was markedly reduced after macrophage depletion (Fig. 6j and Supplementary Fig. 12g). All together, we demonstrate for the first time that targeting of macrophages may represent a novel therapeutic strategy for management of polycythemia vera, a disease commonly thought to be cell-autonomous.

DISCUSSION

Although erythroblastic islands were the first described hematopoietic niche, the *in vivo* relevance of this microenvironment for developing RBCs has been unclear. In this study, we clarify the dual roles that tissue resident macrophages have in RBC production and clearance. Although these antagonistic roles offset in the steady state, we demonstrate that the supportive role of macrophages in RBC development is dominant in recovery from hemolytic anemia, acute blood loss, myeloablation, and also JAK2^{V617F}-induced polycythemia vera.

The delay in erythroid progenitor recovery from hemolytic anemia observed in macrophage-depleted animals is consistent with the impairment previously reported in *Mx1*-Cre;*Itga4*$^{fl/fl}$, *Mx1*-Cre; *Itgb1*$^{fl/fl}$, and Tie2-Cre;*Vcam1*$^{fl/fl}$ animals[30–32]. Together, this indicates that binding of erythroblast integrins to VCAM1 on the central macrophage surface promotes recovery from hemolytic anemia. However, despite the delay in erythroid progenitor recovery, defects in erythroid integrins[31,32] do not impact peripheral erythrocyte recovery from hemolytic anemia to the same extent as macrophage depletion, suggesting additional adhesion-independent mechanisms.

In the myeloablative setting, we observed that depletion of radioresistant host-derived CD169$^+$ macrophages impaired recovery of BM and splenic erythroblasts, which is in line with the tight correlation between the recovery rates of macrophages and erythroid progenitors following allogeneic BMT in humans[33,34]. Antibody blockade of VCAM1 was able to reproduce the delayed BM erythroblast recovery observed in CD169$^+$ macrophage-depleted animals, implicating the structural importance of VCAM1 on the surface of CD169$^+$ macrophages in promoting erythroblast recovery after BMT. Human CD169 has a predicted 72% sequence homology to its murine counterpart, and it can be found on human BM resident, splenic red pulp, and liver macrophages[35]. Here, we report that CD169 and VCAM1 co-expression can also be found on a population of CD15$^-$ CD163$^+$ cells in human BM aspirates with macrophage morphology, indicating a similarly phenotyped population in humans. Subsequent studies will elucidate whether these human CD169$^+$ macrophages share other properties with their murine counterparts.

It has been reported that stress erythropoiesis in mice is dependent on BMP4, which works in concert with stem cell factor, EPO, and hypoxia signals[20]. Flex-tailed mice, which have a mutation in the BMP4 downstream target Smad5, have impaired development of stress erythroid progenitors[36] and display severe impairment in peripheral erythroid recovery from hemolytic anemia[37]. We have observed that clodronate liposome pre-treatment impairs BMP4 induction, delays development of stress BFU-E, and severely compromises peripheral erythroid recovery from hemolytic anemia, which is consistent with the requirement of macrophages to mount BMP4-mediated stress erythropoiesis. We also observed that depletion of CD169$^+$ macrophages following BMT could abrogate the development of BMP4-dependent stress erythropoiesis in the spleen. Since CD169$^+$ macrophage-depleted animals phenocopy the erythroid-specific impairment in recovery post-BMT reported in flex-tailed mice[19,20], this suggests that BMP4 derived from splenic RPM[23] promotes stress erythropoiesis in the spleen. Taken together, this supports a model in which VCAM1 expressed on host-derived BM CD169$^+$ macrophages and BMP4 derived from host-derived splenic RPM work in concert to mediate erythrocyte recovery following myeloablation. Persistent anemia following clinical hematopoietic stem cell transplant is a serious concern with currently no optimal solutions[38,39]. Blood transfusions are associated with iron overload and increased risk of infections, while erythropoietin supplementation does not reduce the number of transfusions required[40]. Thus, strategies to boost CD169$^+$ macrophage recovery following chemotherapy or irradiation-induced injury represents a novel approach to potentially accelerate recovery of the RBC compartment after transplant.

In contrast to myeloablated individuals, patients with PV have a hyperfunctional erythron, resulting in increased blood viscosity and a substantial incidence of thrombosis[41]. The current standard of care treatment for PV patients is still phlebotomy[41]. JAK2 inhibitors to suppress PV are under clinical trials, but are limited at the moment by dose-dependent toxicity and evidence that resistance can develop[42]. In our PV model, we observed unexpectedly that macrophage depletion could normalize the expanded erythron. To our knowledge, this is the first report of BMP4 and stress erythropoiesis contributing to the pathogenesis of PV in mice, and we also show for the first time that macrophage depletion abrogates this erythroid expansion. Importantly, we show that EPO-autonomous colonies, a diagnostic criterion of PV[29], were reduced with macrophage depletion. Thus, our data

indicate that inhibition of the macrophage compartment (e.g. CSF-1 inhibitors[43]) or abrogation of BMP4 may point to new avenues to treat polycythemia vera in addition to phlebotomy and JAK2 inhibitors.

In this study, we clarify the dual roles of macrophages in steady-state erythropoiesis and show their importance in hemolytic anemia, acute blood loss, myeloablative injury, and polycythemia vera. An accompanying manuscript by Rivella and colleagues (Ramos et al.) has independently reached the same conclusions that macrophages are critical in erythroblastic expansion in stress erythropoiesis, and that macrophage targeting can normalize the erythron in polycythemia vera. Together, these two studies strongly support an *in vivo* function for the erythroblastic island and new opportunities for using this knowledge in the treatment of patients with disorders of erythropoiesis.

Online Methods

Mice

All experiments were performed on 8–12 week old animals. C57BL/6 (CD45.2) mice were bred in-house or purchased from Charles River Laboratories (Frederick Cancer Research Center, Frederick, Maryland). For $JAK2^{V617F}$ experiments, C57BL/6-Ly5.2 (CD45.1) animals were purchased from Charles River Laboratories. CD169-DTR[9] heterozygous ($CD169^{DTR/+}$) mice, which were generated with DTR cDNA[44], were bred in-house by crossing $CD169^{DTR/DTR}$ with C57BL/6 mice. With the exception of the $JAK2^{V617F}$ animals, which were housed at the University of Oklahoma Health Sciences Center, all mice were housed in specific pathogen-free facilities at the Mount Sinai School of Medicine or Albert Einstein College of Medicine animal facility. Experimental procedures performed on the mice at each site were approved by the respective Institutional Animal Care and Use Committee of the Mount Sinai School of Medicine or Albert Einstein College of Medicine.

Macrophage depletion

For depletion of $CD169^{+}$ macrophages, heterozygous CD169-DTR ($CD169^{DTR/+}$) were injected i.p. with 10μg/kg DT (Sigma). For steady-state experiments, mice were injected with a single dose of DT or twice weekly for sustained depletion. For PHZ experiments, animals were injected with DT on days −2, 0, 2, 4, and 6 of experiment (PHZ on days 0 and 1). For BMT and 5FU experiments, DT was administered every three days starting one day after BMT or 5FU administration. C57BL/6 mice injected with DT and $CD169^{DTR/+}$ mice not injected with DT both did not demonstrate macrophage depletion and were pooled as control (Ctrl) animals. $CD169^{DTR/+}$ animals injected with DT served as macrophage-depleted experimental mice (DTR). Analysis of macrophage depletion in the $CD169^{DTR/+}$ model beyond six weeks is not possible due to development of immunity to diphtheria toxin (data not shown). In some experiments, macrophages were depleted by injection of PBS- or clodronate-encapsulated liposomes (200μl i.v./infusion). Cl_2MDP (or clodronate) was a gift from Roche Diagnostics (GmbH, Mannheim, Germany). For phenylhydrazine and acute bleeding experiments, a single infusion of liposomes was administered on day −5 of experiment. For PV experiments, a single (day 0 of experiment) or four doses (days 0, 7, 14, 21) were administered as indicated in the text.

CBC analysis

Animals were bled ~25μl via submandibular route into an eppendorf tube containing 1μl of 0.5M EDTA (Fisher). Blood was diluted 1:10 in PBS and ran on Advia counter (Siemens).

Cell preparation

Nucleated single cell suspensions were enriched from peripheral blood, bone marrow, spleen and liver by harvesting interface layer from a lympholyte gradient (Cedar Lane Labs), according to manufacturer's directions. For peripheral blood, 250–500μl of peripheral blood was diluted in 2ml of RPMI media (Cellgro) and carefully pipetted onto 3ml of lympholyte solution in a 15ml tube (Falcon). For BM, femurs were flushed gently with 500μl of ice-cold PBS (Cellgro) through a 1ml syringe (BD) with 21G needle (BD) into an eppendorf tube; then, the entire solution was carefully layered onto 1ml of lympholyte solution in a 5ml polystyrene tube (BD). Spleens were mashed through a 40μm filter (BD) onto a 6 well-plate (BD) containing 4ml of ice-cold PBS. Cell suspension was resuspended to approximately $20x10^6$ cells/ml and 500μl was layered onto 1ml of lympholyte solution in a 5ml polystyrene tube (BD). Liver cells were mechanically diced and digested in a RPMI media (Cellgro) solution containing 0.4mg/ml Type IV collagenase (Sigma) and 10% FBS (Stem Cell Technologies) for 1hr. The liver suspension was drawn through a 3ml syringe (BD) with 19G needle (BD) and filtered through a 40μm filter (BD). The cells were resuspended in 1ml PBS and centrifuged on a 30% Percoll gradient. The supernatant was discarded and the pellet was resuspended in 500μl and was layered onto 1ml of lympholyte solution in a 5ml polystyrene tube (BD). For FACS analyses, RBC lysis with ammonium chloride was not used since some erythroblasts became $DAPI^+$ after lysis.

In vivo isolation of erythroblast islands

Protocol was modified from [3]. Bone marrow was flushed gently with IMDM media (Cellgro) containing 3.5% sodium citrate and 20% FCS solution using an 18G syringe (BD). After pipetting 20 times, 8% of BM by volume (~$1x10^6$ cells) was incubated with F4/80-FITC and Ter119-PE antibody at 1:100 for two hours at room temperature. Cells were then diluted 3.5-fold in FACS buffer containing DAPI and processed by flow cytometry or flow-sorted for the $F4/80^+$ $Ter119^+$ multiplet population by BD FACSAria. Images of erythroblast islands were acquired from glass slides containing 10,000 islands cytospun at 500rpm for 3min with a Cytospin 4 (Thermo Scientific).

Flow cytometry

Fluorochrome-conjugated or biotinylated mAbs specific to mouse Gr-1 (Ly6C/G) (clone RB6-8C5), CD115 (clone AFS98), B220 (clone RA3-6B2), VCAM1 (clone 429), CD11b (clone M1/70), CD45 (clone 30-F11), CD45.1 (clone A20), CD45.2 (clone 104), Ter119 (clone TER-119), CD71 (clone R17217), and CD44 (clone IM7), corresponding isotype controls, and secondary reagents (PerCP-efluor710 and PE-Cy7-conjugated Streptavidin) were purchased from Ebioscience. Anti-F4/80 (clone CI:A3.1) was purchased from AbD Serotec. BrdU incorporation of erythroblasts was assessed in animals injected with 100μg of BrdU i.p. 1 hour prior to harvest and samples were processed according to manufacturer's directions in the APC BrdU Kit (BD Biosciences). In some experiments, APC-conjugated

anti-BrdU (clone Bu20a) from Biolegend was used. Positive staining was gated in reference to cells from mice that were not injected with BrdU. Viable cells were assessed by double negative staining of DAPI (1mg/ml solution diluted to1:20,000) and Annexin V (BD Biosciences). Samples were processed according to manufacturer's directions, but DAPI was substituted for propidium iodide. In some experiments, Alexa Fluor 647 Annexin V was used according to manufacturer's instructions (Biolegend). For nuclear staining in non-permeabilized cells, cell suspensions were incubated 1:1000 with 10mg/ml Hoechst 33342 solution (Sigma) for 45 minutes at 37 C after cell surface staining with other antibodies. For human BM characterization, the following anti-human antibodies were used: VCAM1-PE (clone STA, Biolegend), CD169-Alexa 647 (clone7-239, Biolegend), CD163-biotin (clone eBioGHI/61, Ebioscience), CD15-PerCP-eFluor710 (clone MMA, Ebioscience), and CD14-eFluor450 (clone 61D3, Ebioscience, Biolegend). Multiparameter analyses of stained cell suspensions were performed on an LSRII (BD) and analyzed with FlowJo software (Tree Star). $DAPI^-$ single cells were evaluated for all analyses except for peripheral blood erythroblasts and BrdU assessments.

In vitro culture of erythroblasts

$DAPI^-$ $CD11b^-$ $CD45^-$ $Ter119^+$ $CD71^+$ erythroblasts from wild-type or $CD169^{DTR/+}$ mice were sorted by FACS Aria (BD) and cultured for 24 or 48 hours, as previously described[45] at a concentration of $1x10^5$ sorted cells per 100μl in a 96 well plate (BD). Some wells were incubated with 1μg/ml DT. At 24 and 48 hours after culture, cells were counted and assessed for viability by $Annexin^-$ $DAPI^-$ staining.

Splenectomy

Animals were splenectomized as previously described[46] and allowed to recover at least two weeks prior to the onset of experiments.

Serum erythropoietin

Serum was frozen and assessed by serum EPO ELISA kit (R&D) according to manufacturer's directions.

In vivo biotinylation assay

Mice were injected i.v. with 100mg/kg NHS sulfo-biotin (Thermo Scientific - Pierce) on day 0 and lifespan of RBCs was assessed weekly[47] by staining 1μl of peripheral blood with Streptavidin-PE-Cy7 and gating $CD11b^-CD45^-Ter119^+CD71^-$ cells. For BMT mice, mice were infused with NHS sulfo-biotin 1 day prior to BMT.

Erythroid colony-forming assays

BFU-E (Stem Cell Technologies, M3436) and CFU-E (M3334) of BM cells were plated according to manufacturer's instructions and counted on days 10 and 3 of culture, respectively. Splenic stress BFU-E were assayed by plating $0.5x10^6$ RBC-separated splenocytes in M3436 media and enumerating after 5 days of culture. Endogenous (ie. without EPO) BFU-E and CFU-E were assayed by plating $0.5x10^6$ RBC-separated splenocytes in M3234 media and enumerating after 5 days of culture.

Phenylhydrazine-induced hemolytic anemia

Mice were infused with 40mg/kg phenylhydrazine for two consecutive days, which were considered days 0 and 1 of the experiment. For BMP4 imaging in PHZ-challenged animals, mice were administered a single dose of 40mg/kg of PHZ on day 0 and harvested 24 hours later.

BMP4 immunofluorescence

Spleens were harvested, cut into two halves along the longitudinal axis, fixed for 2h in 4% PFA, then frozen in OCT compound (Sakura), which were subsequently stored at −80°C. 8μm sections were cut onto Superfrost Plus slides and stained with 1:100 F4/80-biotin (clone CI:A3-1, Serotec) and 1:100 polyclonal rabbit anti-mouse BMP4 (Abcam) for 2h. Endogenous biotin was blocked with the Avidin/Biotin blocking kit (Vector Laboratories). After washing for 30 minutes with PBS, slides were stained for 1h with 1:200 Cy5-conjugated Streptavidin (Jackson Labs) and 1:200 Alexa 594-conjugated goat anti-rabbit antibody (Molecular Probes). After washing for 30 minutes with PBS, slides were stained with 2μg/ml DAPI solution for 10 minutes. Images were acquired on a Zeiss Axioplan 2IE equipped with a camera (AxioCam MR).

Acute blood loss

Mice were bled 400μl under isoflurane anesthesia and immediately volume-repleted intraperitoneally with 500μl of PBS on days 0, 1, and 2 of experiment.

Bone marrow transplantation

Mice were irradiated (1,200 cGy, two split doses, 3h apart) in a Cesium Mark 1 irradiator (JL Shepperd & associates). Then, $1x10^6$ RBC-lysed BM nucleated cells were injected retroorbitally under isoflurane (Phoenix pharmaceuticals) anesthesia. Some mice that were depleted with DT and harvested on day 7 were treated intraperitoneally on days 1 and 4 after BMT with 200mg/kg elemental iron (Ferrlecit, sodium ferric gluconate complex in sucrose, Sanofi Aventis). For reciprocal BMT studies, $1x10^6$ WT BM nucleated cells were infused into lethally irradiated WT (WT->WT) or DTR (WT->DTR) mice or $1x10^6$ DTR BM nucleated cells were infused into lethally irradiated WT (WT->DTR) or DTR (DTR->DTR) mice. For polycythemia vera experiments, $3.7x10^6$ RBC-lysed BM cells from C57BL/6 (WT) or $JAK2^{V617F}$ (JAK2) transgenic animals were infused into lethally irradiated C57BL/6-Ly5.2 mice. Mice were allowed to recover 5 weeks or 8 weeks prior to infusion of liposomes. In some experiments, mice were treated intraperitoneally daily with 100mg/kg deferoxamine (Desferal, Novartis).

Quantitative real-time PCR (Q-PCR)

~10,000 RBC-separated splenocytes were lysed in buffer from the Dynabeads RNA Microkit (Invitrogen) in accordance with manufacturer's instructions. Conventional reverse transcription, using the Sprint PowerScript reverse transcriptase (Clontech) was performed in accordance with the manufacturers' instructions. Q-PCR was performed with SYBR GREEN on an ABI PRISM 7900HT Sequence Detection System (Applied Biosystems). The PCR protocol consisted of one cycle at 95°C (10 min) followed by 40 cycles of 95°C (15 s)

and 60°C (1 min). Expression of glyceraldehyde-3-phosphate dehydrogenase (Gapdh) was used as a standard. The average threshold cycle number (CRtR) for each tested mRNA was used to quantify the relative expression of each gene: 2^[Ct(Gapdh)-Ct(gene)]. Primers used are listed below: *Bmp4* (fwd) ATTCCTGGTAACCGAATGCTG, *Bmp4* (rev) CCGGTCTCAGGTATCAAACTAGC, *Gapdh* (fwd) TGTGTCCGTCGTGGATCTGA, *Gapdh* (rev) CCTGCTTCACCACCTTCTTGA.

5-fluorouracil challenge

Mice were injected with 5FU (250mg/kg; Sigma) i.v. under isoflurane (Phoenix pharmaceuticals) anesthesia.

Sternum imaging

Sternal bones were fixed with 4% paraformaldehyde for 30 minutes, blocked with PBS containing 20% normal goat serum (NGS) for three hours, permeabilized with 0.1% Triton X-100 + 5% NGS overnight, permeabilized again with 0.3% Triton X-100 for 2 hours, and then stained with Ter119-PE for two nights. Three washes with PBS for 15 minutes/wash were used between each step. Slides were stained 1:1000 of 10mg/ml Hoechst 33342 for 2 hours immediately prior to image acquisition. Images were acquired using a ZEISS AXIO examiner D1 microscope (Zeiss, Germany) with a confocal scanner unit, CSUX1CU (Yokogawa, Japan) and reconstructed in 3-D with Slide Book software (Intelligent Imaging Innovations).

Microarray

To purify mononuclear phagocyte populations for microarray, we modified the gating strategy from a previously published gating scheme[7]. BM was sorted two times with a FACS Aria sorter (BD) to achieve >99% purity. $Gr1^{hi}$ monocytes were identified by $Gr\text{-}1^{+}CD115^{+}CD3^{-}B220^{-}$. $Gr1^{lo}$ monocytes were identified by $Gr\text{-}1^{-}CD115^{+}F4/80^{+}CD3^{-}B220^{-}$. Macrophages were identified as $Gr1^{-}CD115^{int}F4/80^{+}CD3^{-}B220^{-}SSC^{lo}$. Microarray analysis of sorted cells was performed in collaboration with the Immunological Genome Project (Immgen).

VCAM1 blockade

Mice were infused i.v. with 10mg/kg VCAM1 antibody (clone M/K 2.7) (Bio X Cell) or IgG from rat serum (Sigma) per infusion. For BMT experiments, mice were infused on days 1, 4, 7, 10, and 13 post-BMT.

Characterization of human bone marrow macrophages

Unprocessed fresh human BM aspirates were purchased from Lonza. Leukocytes were purified by harvesting the interface layer after Ficoll (GE Healthcare) separation. Populations were sorted using BSL2-level FACS Aria machine (BD) and cytospun as above. Photomicrographs were acquired using an upright Zeiss AxioPlan II at the MSSM Microscopy Shared Resource Facility.

Iron studies

Serum iron and UIBC were measured using an Iron/TIBC Reagent Set (Pointe Scientific) and transferrin saturation was calculated according to manufacturer's instructions.

Statistical analyses

Unless otherwise indicated in the figure legends, the unpaired Student's *t* test was used in all analyses. Data in bar graphs are represented as mean ± SEM and statistical significance was expressed as follows: *, $P < 0.05$; **, $P < 0.01$; ***, $P < 0.001$; n.s., not significant

Supplementary Material

Refer to Web version on PubMed Central for supplementary material.

Acknowledgments

We would like to acknowledge reagents, technical assistance and guidance provided by Colette Prophete, Neepa Dholakia, the MSSM Microscopy Shared Resource Facility, Jingjing Qi and Seunghee Kim-Schulze at the MSSM Human Immune Monitoring Center, Jordi Ochando and Xuqiang Qiao at the MSSM Flow Cytometry Shared Resource Center, and Lydia Tesfa at the AECOM Flow Cytometry Sorting Facility. This work was supported by the National Institutes of Health grants (R01 grants HL097700; HL069438, DK056638) to PSF, R01CA112100 to MM, and R01HL116340 to PSF and MM. AC, JA, DL, and YK were supported by fellowships from NHLBI (5F30HL099028, AC), the National Institute of General Medical Sciences (T32GM062754, JA), Fundación Ramón Areces (DL), and the Japan Society for the Promotion of Science (YK).

References

1. Bessis M. L' îlot érythroblastique, unité fonctionnelle de la moelle osseuse. Rev Hematol. 1958; 13:8–11. [PubMed: 13555228]
2. Mohandas N, Prenant M. Three-dimensional model of bone marrow. Blood. 1978; 51:633–643. [PubMed: 630113]
3. Lee G, et al. Targeted gene deletion demonstrates that the cell adhesion molecule ICAM-4 is critical for erythroblastic island formation. Blood. 2006; 108:2064–2071. [PubMed: 16690966]
4. Rhodes MM, Kopsombut P, Bondurant MC, Price JO, Koury MJ. Adherence to macrophages in erythroblastic islands enhances erythroblast proliferation and increases erythrocyte production by a different mechanism than erythropoietin. Blood. 2008; 111:1700–1708. [PubMed: 17993612]
5. Hanspal M, Smockova Y, Uong Q. Molecular identification and functional characterization of a novel protein that mediates the attachment of erythroblasts to macrophages. Blood. 1998; 92:2940–2950. [PubMed: 9763581]
6. Chasis JA, Mohandas N. Erythroblastic islands: niches for erythropoiesis. Blood. 2008; 112:470–478. [PubMed: 18650462]
7. Chow A, et al. Bone marrow CD169+ macrophages promote the retention of hematopoietic stem and progenitor cells in the mesenchymal stem cell niche. The Journal of experimental medicine. 2011; 208:261–271. [PubMed: 21282381]
8. Chow A, Brown BD, Merad M. Studying the mononuclear phagocyte system in the molecular age. Nature reviews Immunology. 2011; 11:788–798.
9. Miyake Y, et al. Critical role of macrophages in the marginal zone in the suppression of immune responses to apoptotic cell-associated antigens. J Clin Invest. 2007; 117:2268–2278. [PubMed: 17657313]
10. Crocker PR, Werb Z, Gordon S, Bainton DF. Ultrastructural localization of a macrophage-restricted sialic acid binding hemagglutinin, SER, in macrophage-hematopoietic cell clusters. Blood. 1990; 76:1131–1138. [PubMed: 2205308]
11. Manwani D, Bieker JJ. The erythroblastic island. Current topics in developmental biology. 2008; 82:23–53. [PubMed: 18282516]

12. Barbe E, Huitinga I, Dopp EA, Bauer J, Dijkstra CD. A novel bone marrow frozen section assay for studying hematopoietic interactions in situ: the role of stromal bone marrow macrophages in erythroblast binding. Journal of cell science. 1996; 109 (Pt 12):2937–2945. [PubMed: 9013341]
13. Ramos P, et al. Enhanced erythropoiesis in Hfe-KO mice indicates a role for Hfe in the modulation of erythroid iron homeostasis. Blood. 2011; 117:1379–1389. [PubMed: 21059897]
14. Schroit AJ, Madsen JW, Tanaka Y. In vivo recognition and clearance of red blood cells containing phosphatidylserine in their plasma membranes. The Journal of biological chemistry. 1985; 260:5131–5138. [PubMed: 3988747]
15. Sadahira Y, et al. Impaired splenic erythropoiesis in phlebotomized mice injected with CL2MDP-liposome: an experimental model for studying the role of stromal macrophages in erythropoiesis. J Leukoc Biol. 2000; 68:464–470. [PubMed: 11037966]
16. Bessis M. Erythroblastic island functional unity of bone marrow. Rev Hematol. 1958; 13:8–11. [PubMed: 13555228]
17. Cairo G, Recalcati S, Mantovani A, Locati M. Iron trafficking and metabolism in macrophages: contribution to the polarized phenotype. Trends in immunology. 2011; 32:241–247. [PubMed: 21514223]
18. Zhang Z, et al. Ferroportin1 deficiency in mouse macrophages impairs iron homeostasis and inflammatory responses. Blood. 2011; 118:1912–1922. [PubMed: 21705499]
19. Harandi OF, Hedge S, Wu DC, McKeone D, Paulson RF. Murine erythroid short-term radioprotection requires a BMP4-dependent, self-renewing population of stress erythroid progenitors. J Clin Invest. 2010; 120:4507–4519. [PubMed: 21060151]
20. Paulson RF, Shi L, Wu DC. Stress erythropoiesis: new signals and new stress progenitor cells. Curr Opin Hematol. 2011; 18:139–145. [PubMed: 21372709]
21. Hashimoto D, et al. Pretransplant CSF-1 therapy expands recipient macrophages and ameliorates GVHD after allogeneic hematopoietic cell transplantation. The Journal of experimental medicine. 2011; 208:1069–1082. [PubMed: 21536742]
22. Sadahira Y, Mori M, Kimoto T. Participation of radioresistant Forssman antigen-bearing macrophages in the formation of stromal elements of erythroid spleen colonies. Br J Haematol. 1989; 71:469–474. [PubMed: 2653405]
23. Millot S, et al. Erythropoietin stimulates spleen BMP4-dependent stress erythropoiesis and partially corrects anemia in a mouse model of generalized inflammation. Blood. 2010; 116:6072–6081. [PubMed: 20844235]
24. Sadahira Y, Yoshino T, Monobe Y. Very late activation antigen 4-vascular cell adhesion molecule 1 interaction is involved in the formation of erythroblastic islands. The Journal of experimental medicine. 1995; 181:411–415. [PubMed: 7528776]
25. Kohyama M, et al. Role for Spi-C in the development of red pulp macrophages and splenic iron homeostasis. Nature. 2009; 457:318–321. [PubMed: 19037245]
26. Gooi HC, et al. Marker of peripheral blood granulocytes and monocytes of man recognized by two monoclonal antibodies VEP8 and VEP9 involves the trisaccharide 3-fucosyl-N-acetyllactosamine. Eur J Immunol. 1983; 13:306–312. [PubMed: 6189722]
27. Tippett E, et al. Differential expression of CD163 on monocyte subsets in healthy and HIV-1 infected individuals. Plos One. 2011; 6:e19968. [PubMed: 21625498]
28. Xing S, et al. Transgenic expression of JAK2V617F causes myeloproliferative disorders in mice. Blood. 2008; 111:5109–5117. [PubMed: 18334677]
29. Tefferi A, et al. Proposals and rationale for revision of the World Health Organization diagnostic criteria for polycythemia vera, essential thrombocythemia, and primary myelofibrosis: recommendations from an ad hoc international expert panel. Blood. 2007; 110:1092–1097. [PubMed: 17488875]
30. Scott LM, Priestley GV, Papayannopoulou T. Deletion of alpha4 integrins from adult hematopoietic cells reveals roles in homeostasis, regeneration, and homing. Mol Cell Biol. 2003; 23:9349–9360. [PubMed: 14645544]
31. Ulyanova T, Jiang Y, Padilla S, Nakamoto B, Papayannopoulou T. Combinatorial and distinct roles of alpha and alpha integrins in stress erythropoiesis in mice. Blood. 2011; 117:975–985. [PubMed: 20956802]

32. Bungartz G, et al. Adult murine hematopoiesis can proceed without beta1 and beta7 integrins. Blood. 2006; 108:1857–1864. [PubMed: 16735603]
33. Thiele J, et al. Macrophages and their subpopulations following allogenic bone marrow transplantation for chronic myeloid leukaemia. Virchows Archiv : an international journal of pathology. 2000; 437:160–166. [PubMed: 10993276]
34. Thiele J, et al. Erythropoietic reconstitution, macrophages and reticulin fibrosis in bone marrow specimens of CML patients following allogeneic transplantation. Leukemia. 2000; 14:1378–1385. [PubMed: 10942232]
35. Hartnell A, et al. Characterization of human sialoadhesin, a sialic acid binding receptor expressed by resident and inflammatory macrophage populations. Blood. 2001; 97:288–296. [PubMed: 11133773]
36. Lenox LE, Perry JM, Paulson RF. BMP4 and Madh5 regulate the erythroid response to acute anemia. Blood. 2005; 105:2741–2748. [PubMed: 15591122]
37. Coleman DL, Russell ES, Levin EY. Enzymatic studies of the hemopoietic defect in flexed mice. Genetics. 1969; 61:631–642. [PubMed: 5393940]
38. Seggewiss R, Einsele H. Hematopoietic growth factors including keratinocyte growth factor in allogeneic and autologous stem cell transplantation. Semin Hematol. 2007; 44:203–211. [PubMed: 17631184]
39. Miller CB, et al. Impaired erythropoietin response to anemia after bone marrow transplantation. Blood. 1992; 80:2677–2682. [PubMed: 1421381]
40. Heuser M, Ganser A. Recombinant human erythropoietin in the treatment of nonrenal anemia. Ann Hematol. 2006; 85:69–78. [PubMed: 16078035]
41. Zhan H, Spivak JL. The diagnosis and management of polycythemia vera, essential thrombocythemia, and primary myelofibrosis in the JAK2 V617F era. Clinical advances in hematology & oncology : H&O. 2009; 7:334–342. [PubMed: 19521323]
42. Reddy MM, Deshpande A, Sattler M. Targeting JAK2 in the therapy of myeloproliferative neoplasms. Expert opinion on therapeutic targets. 2012; 16:313–324. [PubMed: 22339244]
43. Hume DA, MacDonald KP. Therapeutic applications of macrophage colony-stimulating factor-1 (CSF-1) and antagonists of CSF-1 receptor (CSF-1R) signaling. Blood. 2012; 119:1810–1820. [PubMed: 22186992]
44. Saito M, et al. Diphtheria toxin receptor-mediated conditionaland targeted cell ablation in transgenic mice. Nature biotechnology. 2001; 19:746–750.
45. Chen K, et al. Resolving the distinct stages in erythroid differentiation based on dynamic changes in membrane protein expression during erythropoiesis. Proc Natl Acad Sci U S A. 2009; 106:17413–17418. [PubMed: 19805084]
46. Reeves JP, Reeves PA, Chin LT. Survival surgery: removal of the spleen or thymus. Current protocols in immunology/edited by John E Coligan [et al]. 2001; Chapter 1(Unit 1):10.
47. Hoffmann-Fezer G, et al. Biotin labeling as an alternative nonradioactive approach to determination of red cell survival. Annals of Hematology. 1993; 67:81–87. [PubMed: 8347734]

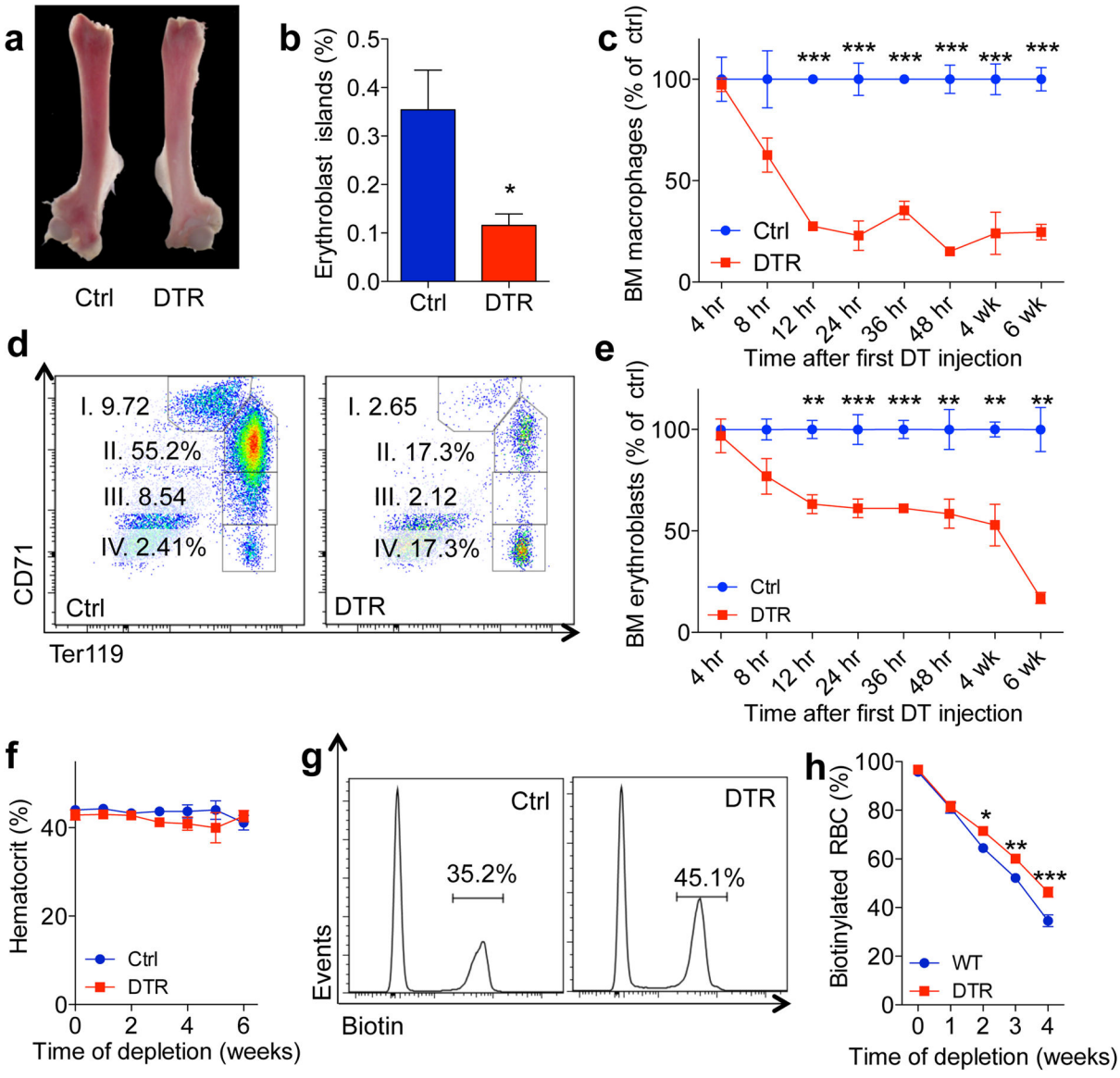

Figure 1. Depletion of bone marrow CD169^{+} macrophages results in reduced erythroblast numbers without peripheral blood anemia

a) Photomicrograph of femurs dissected from wild-type (Ctrl) or CD169$^{DTR/+}$ (DTR) treated with DT for 4 weeks. b) Percentage of F4/80^{+} Ter119^{+} multiplets (Erythroblast islands) in femurs of Ctrl and DTR mice (n=5). c) Quantitation of BM macrophages at various time points of depletion (n=3–18). Absolute numbers of macrophages per femur were normalized such that average values of Ctrl mice were set at 100% at each time point. d) Flow cytometry plots of DAPI^{-} CD11b^{-} CD45^{-} single cells from BM of Ctrl or DTR mice. e) Quantitation of BM erythroblasts (sum of populations I–IV of d) at various time points of depletion (n=3–18). Absolute numbers of erythroblasts per femur were normalized such that average values of Ctrl mice were set at 100% at each time point. f) Hematocrit measurement from circulating blood after CD169^{+} macrophage depletion over 6 weeks (n=9–14, pooled from three independent experiments). g) Representative FACS plot and h) quantitation of

percentage of DAPI^{-} CD11b^{-} CD45^{-} Ter119^{+} CD71^{-} single cells in peripheral blood that were biotin^{+} during weekly bleeding of Ctrl and DTR mice (n=5, representative of two independent experiments).

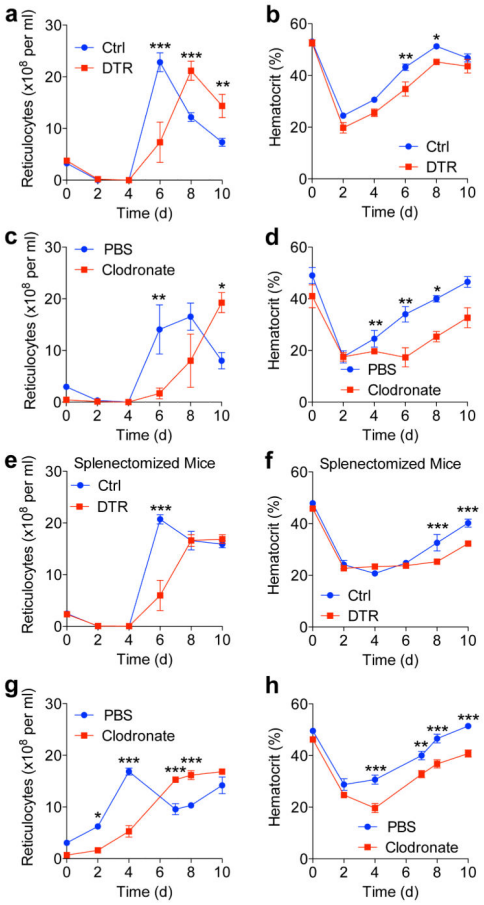

Figure 2. Depletion of macrophages impairs erythroid recovery after hemolytic anemia and acute blood loss

a–b) Reticulocyte and hematocrit assessments in Ctrl and DTR mice following induction of hemolytic anemia with phenylhydrazine on days 0 and 1 (n=10, pooled from two independent experiments). c–d) Reticulocyte and hematocrit assessments in PBS and clodronate liposome-treated mice following induction of hemolytic anemia with phenylhydrazine (n=4, representative of two independent experiments). e–f) Reticulocyte and hematocrit assessments in splenectomized Ctrl and DTR mice following induction of hemolytic anemia with phenylhydrazine (n=7–11, pooled from two independent experiments). g–h) Reticulocyte and hematocrit assessments in PBS and clodronate liposome-treated mice following acute bleeding on days 0, 1, and 2 (n=5).

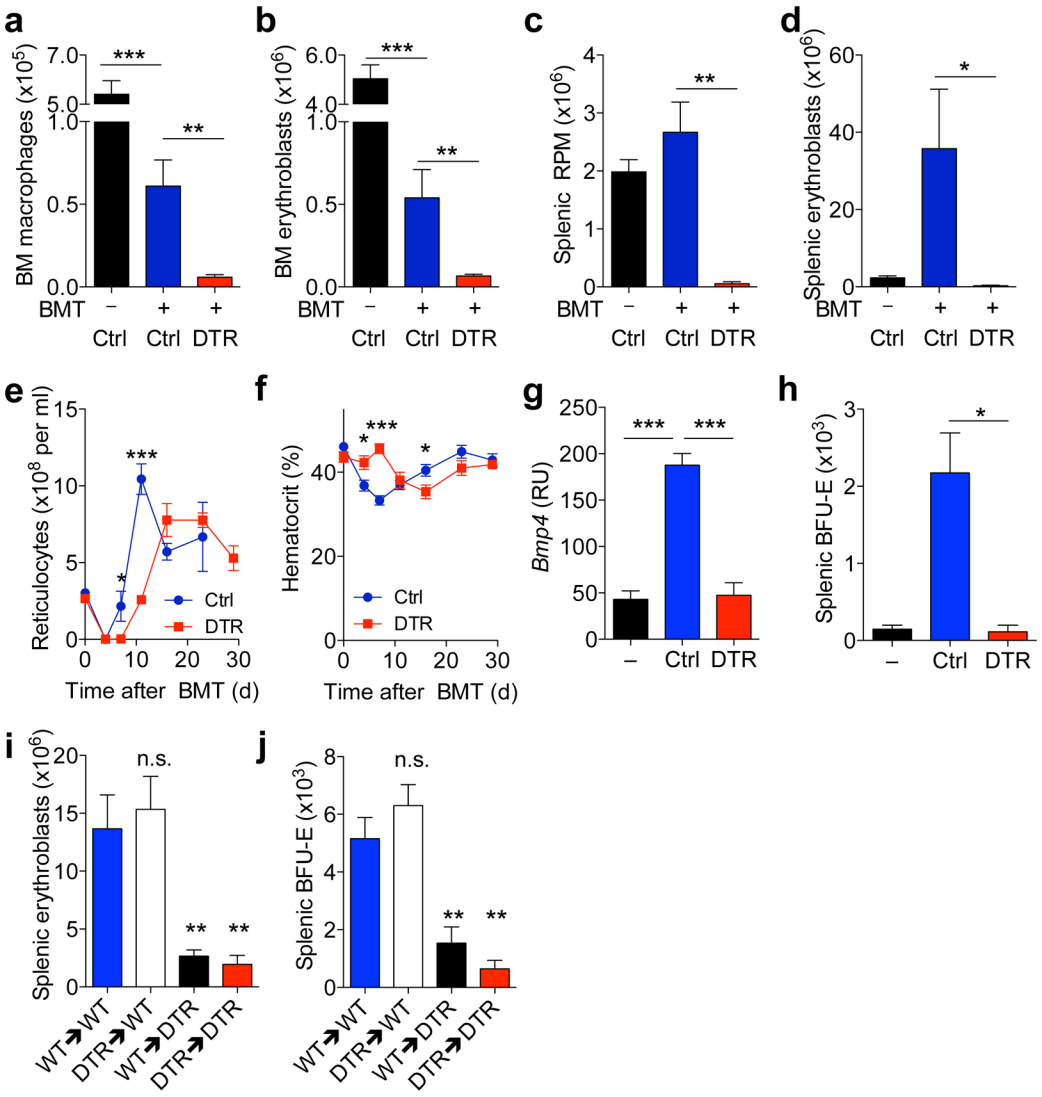

Figure 3. Depletion of macrophages impairs erythroid recovery after myeloablation

a–d) Macrophage (a,c) and erythroblast (b,d) counts per femur (a,b) and spleen (c,d) of Ctrl (blue) and DTR (red) animals 7 days after transplantation of 1x10^6 BM cells. Untransplanted animals (black) are displayed for comparison (BM: n=7–10, pooled from two independent experiments; spleen: n=4–5). e–f) Reticulocyte and hematocrit assessments following transplantation of 1x10^6 BM cells (n=20, pooled from five independent experiments). g) Gene expression of *Bmp4* and h) stress BFU-E in spleens of untransplanted (black), Ctrl (blue), and DTR (red) animals 7 days after BMT (n=3–4). RU=(10^6) (expression relative to *Gapdh*). i–j) Quantitation of splenic i) erythroblasts and j) stress BFU-E in reciprocally-transplanted and DT-treated mice 7 days after BMT (n=5).

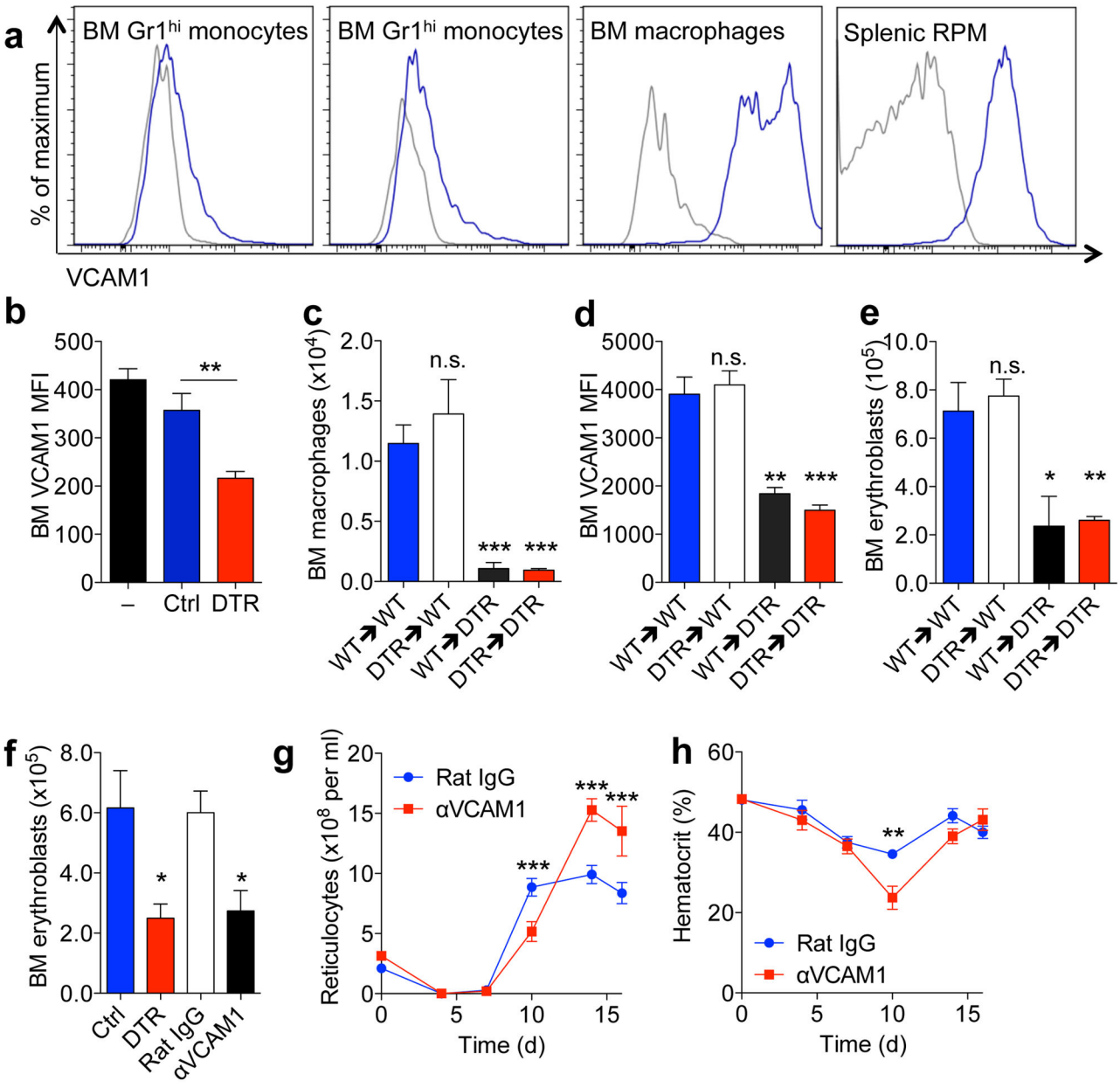

Figure 4. VCAM1 blockade abrogates bone marrow erythroblast recovery

a) FACS plots of surface-bound VCAM1 levels on BM monocytes, BM macrophages and splenic red pulp macrophages (blue = VCAM1, gray = isotype control). b) VCAM1 levels (mean fluorescent intensity, MFI) on BM DAPI^{-} single cells in untransplanted animals (black) or 7d after BMT in Ctrl (blue) and DTR (red) mice (n=4–5, representative of two independent experiments). c–e) Quantitation of BM c) macrophages per femur, d) VCAM1 MFI and e) erythroblast numbers in reciprocally-transplanted and DT-treated mice 7d after BMT (n=5). f) BM erythroblast numbers 7d after BMT of Ctrl (blue), DTR (full red), rat IgG-treated (white) or anti-VCAM1-treated (black) animals (n=3–4). g–h) Reticulocyte and hematocrit assessments in rat IgG-treated (blue) or anti-VCAM1 (red) animals following BMT (n=10).

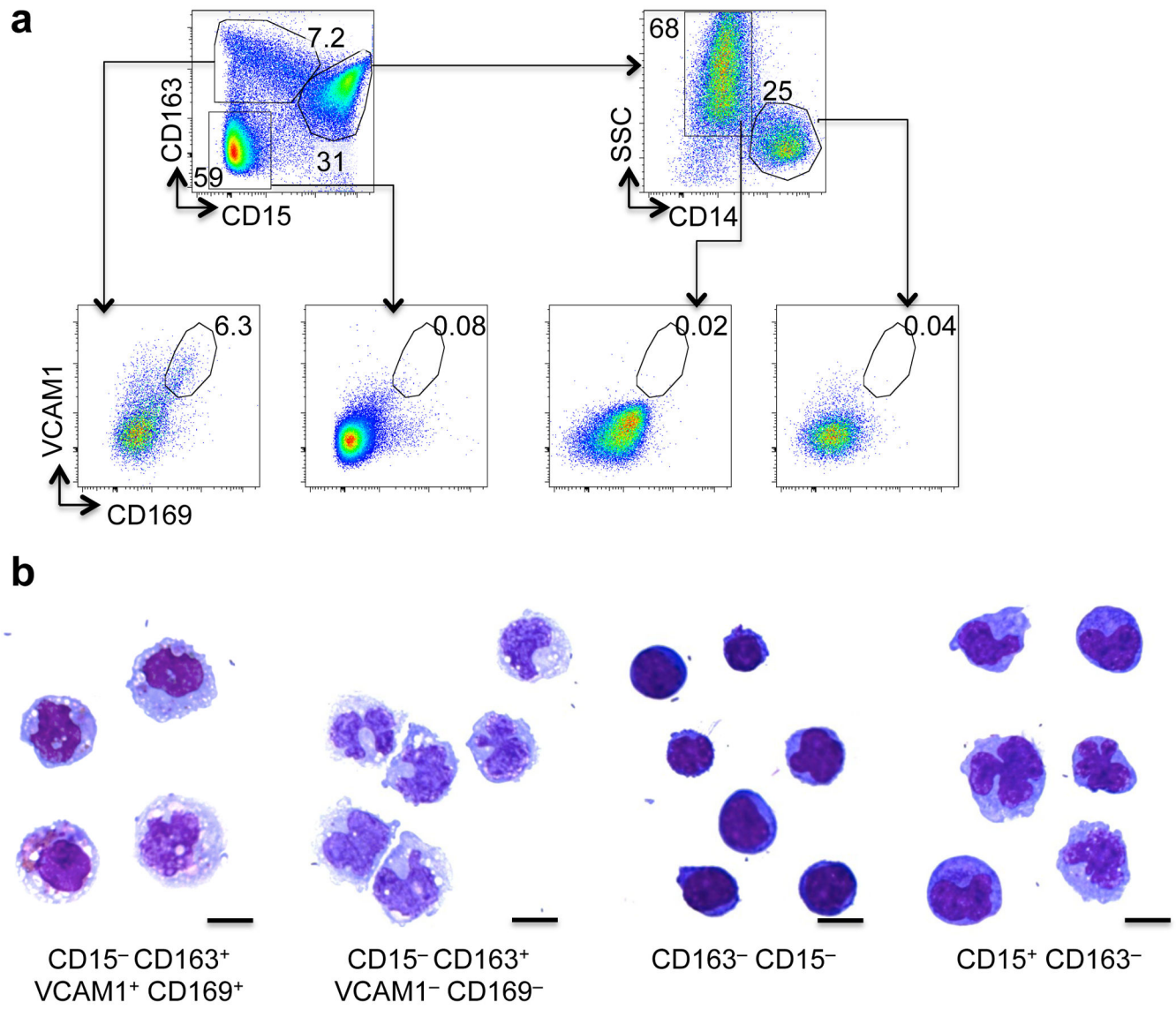

Figure 5. CD15^{-} CD163^{+} CD169^{+} marks a population of human macrophages expressing VCAM1

a) FACS plots of subpopulations of CD45^{+} cells from a healthy human BM aspirate sample distinguished by differential expression of CD163, CD15, CD14, CD169, and VCAM1. Representative data from two independent samples are shown. b) Compiled photomicrographs of populations that were sorted as indicated and cytospun. Scale bar = 10μm.

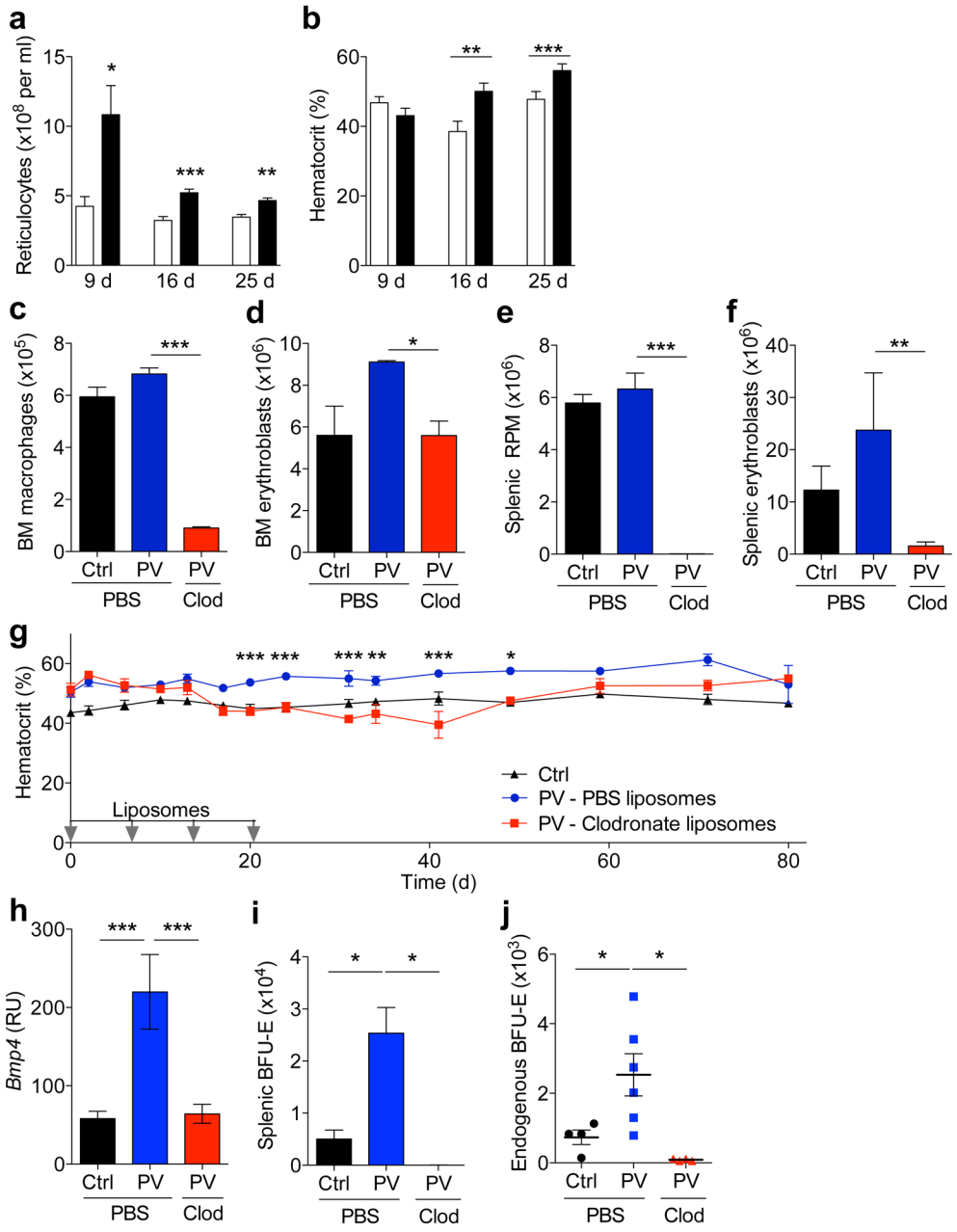

Figure 6. Depletion of macrophages normalizes the erythroid compartment in a JAK2^{V617F}-induced murine model of polycythemia vera

a,b) Erythroid parameters from circulating blood counts at 9, 16 and 25 d after transplantation of 3.7x10^6 wild-type (white, Ctrl) or JAK2^{V617F} (black, PV) bone marrow cells (n=10, pooled from two independent experiments). c–f) Macrophage (c,e) and erythroblast (d,f) counts per femur (c,d) and spleen (e,f) 7 d after last of four weekly infusions of liposomes (day 28 of experiment, 9 weeks post-BMT) into Ctrl or PV animals (n=3). g) Hematocrit levels of Ctrl (black) or PV mice that were treated with PBS (blue) or clodronate (red) liposomes (n=11–13, pooled from two independent experiments). Data analysed with two-way ANOVA with Bonferroni post-test. Day 0 corresponds to first day of

liposome injection and 5 weeks after BMT. Liposomes were injected on days 0, 7, 14 and 21 (grey arrows). h–j) Quantitation of h) gene expression of *Bmp4*, i) stress BFU-E, and j) endogenous BFU-E in spleens of Ctrl (black) and PV mice treated with PBS (blue) or clodronate (red) liposomes (n=4–6) and harvested on day 30 of experiment. RU=(10^6) (expression relative to *Gapdh*). Day 0 corresponds to first day of liposome injection and 8 weeks after BMT. Liposomes were injected on days 0, 7, 14 and 21.